

Cancer drug addiction is relayed by an ERK2-dependent phenotype switch

Xiangjun Kong¹, Thomas Kuilman¹, Aida Shahrabi¹, Julia Boshuizen¹, Kristel Kemper¹, Ji-Ying Song², Hans W. M. Niessen³, Elisa A. Rozeman¹, Marnix H. Geukes Foppen¹, Christian U. Blank¹ & Daniel S. Peeper¹

Observations from cultured cells^{1–3}, animal models⁴ and patients^{5–7} raise the possibility that the dependency of tumours on the therapeutic drugs to which they have acquired resistance represents a vulnerability with potential applications in cancer treatment. However, for this drug addiction trait to become of clinical interest, we must first define the mechanism that underlies it. We performed an unbiased CRISPR–Cas9 knockout screen on melanoma cells that were both resistant and addicted to inhibition of the serine/threonine-protein kinase BRAF, in order to functionally mine their genome for ‘addiction genes’. Here we describe a signalling pathway comprising ERK2 kinase and JUNB and FRA1 transcription factors, disruption of which allowed addicted tumour cells to survive on treatment discontinuation. This occurred in both cultured cells and mice and was irrespective of the acquired drug resistance mechanism. In melanoma and lung cancer cells, death induced by drug withdrawal was preceded by a specific ERK2-dependent phenotype switch, alongside transcriptional reprogramming reminiscent of the epithelial–mesenchymal transition. In melanoma cells, this reprogramming caused the shutdown of microphthalmia-associated transcription factor (MITF), a lineage survival oncoprotein; restoring this protein reversed phenotype switching and prevented the lethality associated with drug addiction. In patients with melanoma that had progressed during treatment with a BRAF inhibitor, treatment cessation was followed by increased expression of the receptor tyrosine kinase AXL, which is associated with the phenotype switch. Drug discontinuation synergized with the melanoma chemotherapeutic agent dacarbazine by further suppressing MITF and its prosurvival target, B-cell lymphoma 2 (BCL-2), and by inducing DNA damage in cancer cells. Our results uncover a pathway that underpins drug addiction in cancer cells, which may help to guide the use of alternating therapeutic strategies for enhanced clinical responses in drug-resistant cancers.

We treated a panel of four BRAF^{V600E} melanoma cell lines with the BRAF inhibitor (BRAFi) dabrafenib or with dabrafenib in combination with the MEK inhibitor (MEKi) trametinib. As expected, all cell lines were highly sensitive to these drugs (Fig. 1a). After 3–5 months of treatment, pools of cells emerged that had developed resistance to the lethal drug dose (these were labelled BR, for cells resistant to BRAFi, and BMR for cells resistant to the combined BRAFi and MEKi). However, when we acutely discontinued these drug treatments, the drug-resistant cells suffered massive mortality (Fig. 1b and Extended Data Fig. 1): they had become addicted to the very drugs that initially served to eliminate them.

To functionally screen for genes that are essential in developing this drug addiction, we introduced a lentiviral genome-wide CRISPR–Cas9 knockout (GeCKO) library⁸ into drug-treated and addicted 451Lu^{BR} cells (Fig. 1c). Thirty days after drug withdrawal, 13 clones emerged, which appeared to have lost the drug addiction phenotype.

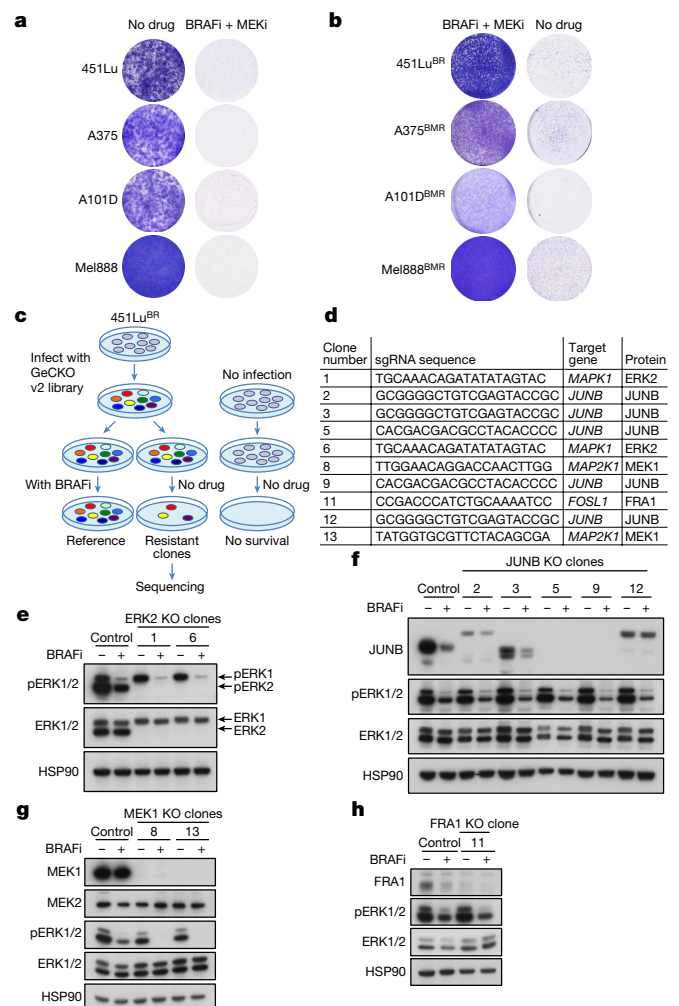


Figure 1 | Genome-wide CRISPR–Cas9 knockout screen to break cancer drug addiction identifies several signalling pathway components.

a, BRAF mutant melanoma cells treated with 1 μ M dabrafenib (451Lu cells) or 0.5 μ M dabrafenib + 0.05 μ M trametinib (A375, A101D and Mel888 cells) and stained 10 days later. **b**, BRAFi-resistant 451Lu^{BR} cells were cultured with or without 1 μ M dabrafenib; BRAFi + MEKi-resistant A375^{BMR}, A101D^{BMR} and Mel888^{BMR} cells were cultured with or without 0.5 μ M dabrafenib + 0.05 μ M trametinib and stained after two (treated) or three weeks (untreated). **c**, **d**, Screen outline and hits for which the same target gene was found in more than two independent screen clones. **e–h**, Control cells and screen clones (as indicated), after dabrafenib or no treatment, were analysed by immunoblotting. KO, knockout. For gel source images, see Supplementary Fig. 1. Data in **a**, **b**, **e–h** are representative of three independent biological experiments.

¹Division of Molecular Oncology and Immunology, The Netherlands Cancer Institute, Plesmanlaan 121, 1066 CX Amsterdam, The Netherlands. ²Division of Experimental Animal Pathology, The Netherlands Cancer Institute, Plesmanlaan 121, 1066 CX Amsterdam, The Netherlands. ³Department of Pathology and Cardiac Surgery, VU University Medical Center, ACS, 1007 MB Amsterdam, The Netherlands.

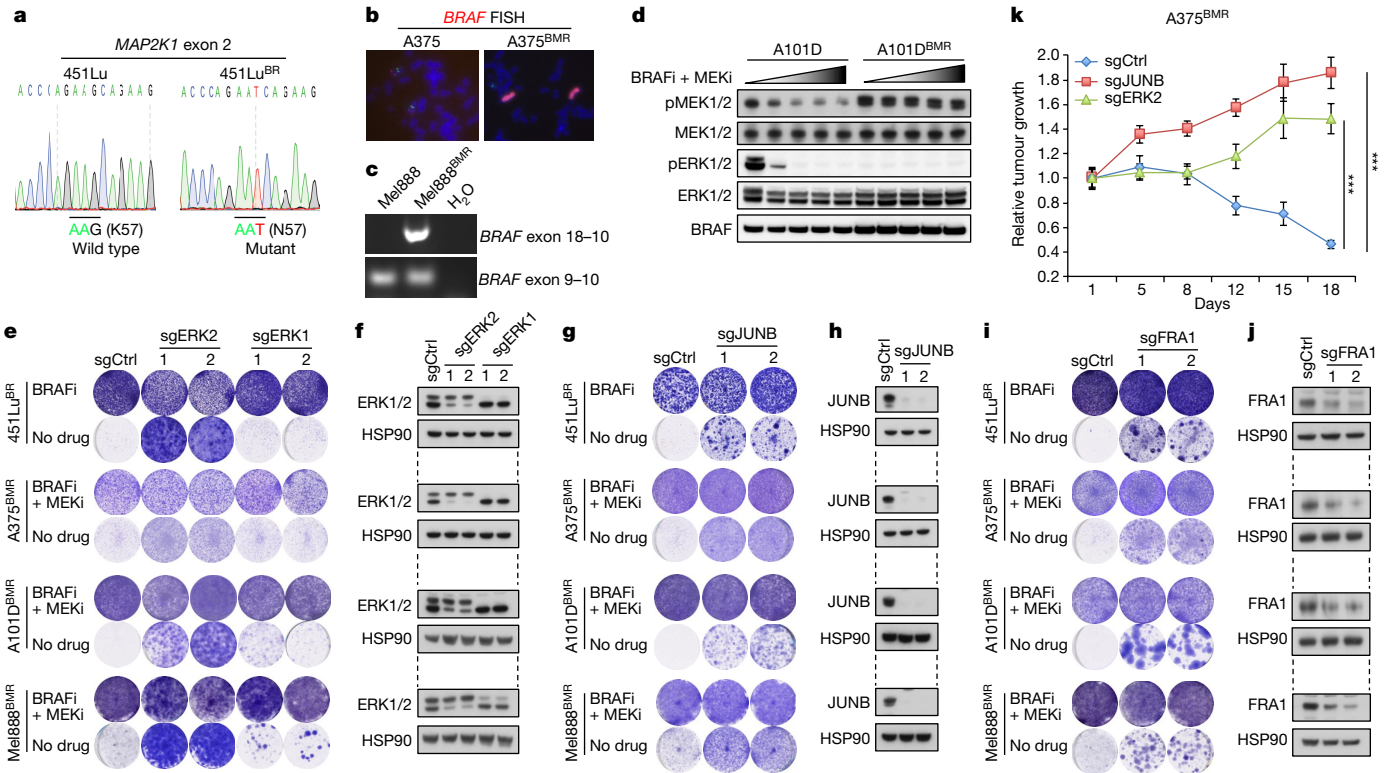


Figure 2 | Conserved drug addiction pathway in multiple cell lines with distinct therapy resistance mechanisms. **a**, *MAP2K1* exon 2 sequence of 451Lu and 451Lu^{BR} cells. **b**, Fluorescence *in situ* hybridization (FISH) performed on metaphase spreads of A375 and A375^{BMR} cells using probes for *BRAF* (red) and a chromosome 7 centromeric region (green). **c**, PCR with reverse transcription performed on cDNA from Mel888 and Mel888^{BMR} cells using *BRAF* exon 18 forward and exon 10 reverse primers. A *BRAF* exon 9–10 amplification serves as a control. **d**, A101D and A101D^{BMR} cells were treated with increasing concentrations of dabrafenib + trametinib (0 + 0 μ M, 0.01 + 0.001 μ M, 0.1 + 0.01 μ M, 1 + 0.1 μ M and 10 + 1 μ M) for six hours and immunoblotted. **e–j**, A melanoma cell line panel was infected with lentivirus expressing sgRNAs targeting the indicated genes or a control

For nine of these, we identified single-guide RNAs (sgRNAs) for the same gene in two or more individual clones (Fig. 1d; for full sequencing data, see Supplementary Table 1); these sgRNAs targeted genes that encode several factors known to communicate with one another, namely ERK2, JUNB and MEK1. We also included FRA1, a partner of JUNB, in further analyses. A first validation round confirmed that the sgRNAs had caused the expected perturbations of genes encoding ERK2 (with intact ERK1; Fig. 1e), JUNB (Fig. 1f), MEK1 (with intact MEK2; Fig. 1g) and FRA1 (Fig. 1h). This genome-wide perturbation screen was therefore able to successfully identify a signalling pathway responsible for the drug addiction phenotype.

To determine whether these screen hits operated in a general fashion, we used a panel of melanoma cell lines that had acquired drug resistance through distinct mechanisms: 451Lu^{BR} cells showed hyperactivation of the ERK pathway (Extended Data Fig. 2a) and harboured a MEK1^{K57N}-activating mutation (Fig. 2a); A375^{BMR} cells, which carry a *BRAF* amplification, also displayed boosted MEK–ERK signalling (Fig. 2b and Extended Data Fig. 2b, c); and Mel888^{BMR} cells showed hyperactivated MEK–ERK signalling and harboured a kinase domain duplication (Fig. 2c and Extended Data Fig. 2d), as recently described⁹. By contrast, A101D^{BMR} cells acquired drug resistance without detectable ERK reactivation (Fig. 2d).

In control drug-addicted melanoma cells, drug withdrawal was accompanied by massive cell death; however, knocking out *MAPK1* (encoding ERK2) resulted in a vigorous rescue across the entire cell panel (Fig. 2e, f). By contrast, genetic perturbation of *MAPK3*

(encoding ERK1) failed to prevent drug addiction. As with ERK2, inactivation of *JUNB* (Fig. 2g, h) or loss of *FOSL1* (encoding FRA1; Fig. 2i, j) generally rescued the cell death associated with withdrawal in drug-addicted cells. Knocking out *MAP2K1* (encoding MEK1) also prevented drug addiction, but only in 451Lu^{BR} cells (Extended Data Fig. 3a, b); the resistance mechanism of this cell line, a MEK1^{K57N}-activating mutation (Figs 1g, 2a), renders it susceptible to breaking drug addiction upon loss of MEK1. The ERK2–JUNB–FRA1 pathway was, therefore, validated across a heterogeneous cell line panel, suggesting a common mechanism of action for drug addiction, which is independent of how cells achieve therapy resistance.

To determine whether the drug addiction phenotype manifests *in vivo*, we established melanoma xenografts in mice in the presence of both dabrafenib and trametinib. When treatment ceased, control tumours regressed; JUNB and ERK2-knockout tumours, however, continued to expand (Fig. 2k), indicating that the drug addiction phenotype is also seen in tumours.

These findings implicated ERK2 signalling in the sensitivity of drug-resistant cells to treatment discontinuation. In 451Lu^{BR}, A375^{BMR} and Mel888^{BMR} cells, we observed hyperactivation of MEK–ERK signalling upon drug withdrawal, a so-called rebound signal (Extended Data Fig. 4a). A101D^{BMR} cells, which have acquired resistance to BRAF–MEK inhibition in an ERK-independent fashion (Fig. 2d), showed an equally intense ERK rebound upon drug washout. This result suggests that the mechanism of acquiring drug resistance is uncoupled from the signalling pathway that manifests drug addiction.

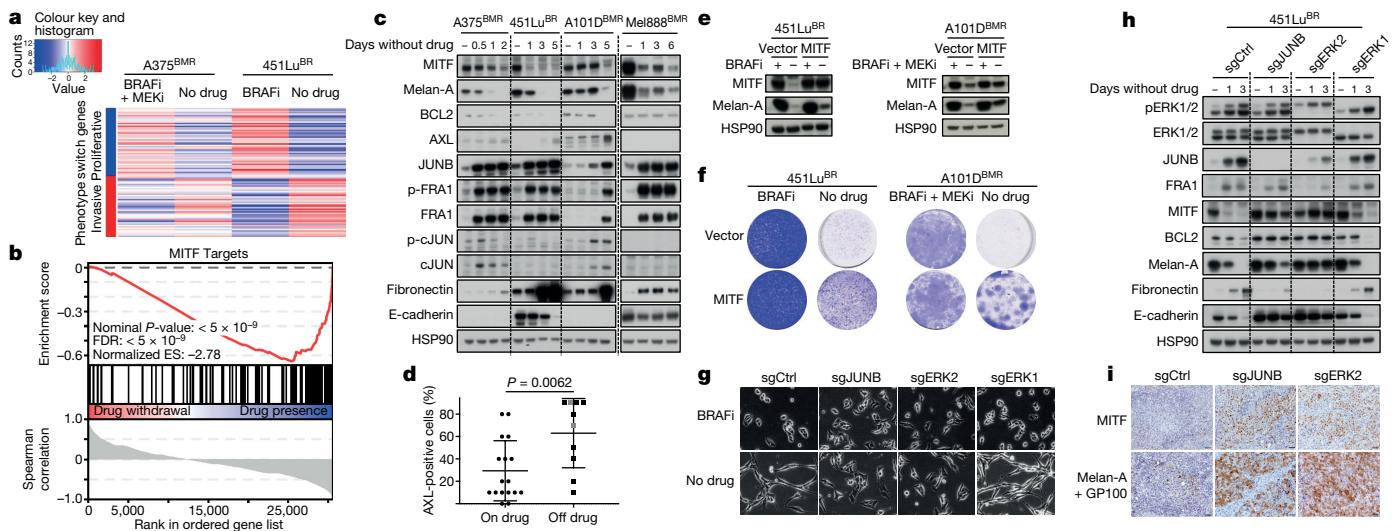


Figure 3 | ERK2 and JUNB act in an MITF-dependent genetic phenotype switch that controls drug addiction. **a**, A375^{BMR} cells were cultured with 0.5 μ M dabrafenib + 0.05 μ M trametinib, or without drugs, for 6, 24 and 48 hours, and 451Lu^{BR} cells were cultured with 1 μ M dabrafenib, or without drugs, for 1, 3 and 5 days, and then analysed for RNA expression. Phenotype switch genes were selected from the sequence data and the t_0 and last time points are represented in a heat map. **b**, Sequence data from **a** (all time points) were subjected to GSEA. For P value calculation, see Methods. **c**, Drug-addicted melanoma cell line panel was cultured with or without MAPK pathway inhibitors for the indicated amount of time, and then immunoblotted. **d**, AXL immunostaining of a sample cohort of BRAFi-resistant melanomas, on ($n = 17$) or off ($n = 10$) treatment. Samples in the ‘off drug’ group were

Corroborating these findings, a low dose of ERK inhibitor completely prevented lethality stemming from drug withdrawal, not only in the three cell lines with ERK rebound (consistent with previous results³) but also in A101D^{BMR} cells (Extended Data Fig. 4b). Thus, regardless of the resistance mechanism, melanoma cells show ERK rebound upon drug withdrawal, which contributes to the drug addiction trait.

As our screen identified two key signalling transcription factors (JUNB and FRA1), we investigated whether drug addiction is relayed by transcriptional reprogramming. RNA profiling of drug-addicted cells after drug cessation revealed a common expression alteration for the top 200 variant genes in two cell lines (Extended Data Fig. 5a). This was accompanied by a major switch in the activity of genes involved in cell proliferation and in those contributing to cell invasion, reminiscent of changes seen for phenotype switching (transcriptional and phenotypic plasticity between alternative proliferative and invasive states)^{10–12} (Fig. 3a).

MITF is a pivotal transcription factor that drives the specification and survival of the melanocytic lineage¹³ and has a central role in melanoma phenotype switching¹¹. Gene set enrichment analysis (GSEA) revealed a strong negative association between drug withdrawal and MITF signature (Fig. 3b), with many MITF targets being strongly downregulated upon drug withdrawal. GSEA confirmed that the transcriptional signatures of AP-1, TEAD and JUNB¹⁴ were enriched upon drug withdrawal (Extended Data Fig. 5b), further supporting the notion that drug-addicted cells underwent phenotype switching after drug withdrawal.

MITF protein levels concordantly declined upon drug withdrawal in all four cell lines examined (Fig. 3c). As a result, both the MITF-controlled Melan-A and BCL-2 proteins were downregulated. Drug withdrawal was also associated with the upregulation of fibronectin and downregulation of E-cadherin, two EMT proteins. MITF expression has recently been shown to be inversely correlated with the expression of the receptor tyrosine kinase AXL^{15,16}. Consistent with this, AXL was induced by drug removal, as were JUNB and FRA1 (Fig. 3c).

taken a maximum of three months after drug discontinuation. Two patients (indicated in grey) had received a first cycle of ipilimumab at the time of biopsy; the other patients had not received any treatment at time of biopsy. Data in graphs are mean \pm s.d. P value calculated by two-sided Mann–Whitney test (confidence interval 95%). **e**, **f**, Cells expressing empty vector or *MITF* cDNA were cultured with or without inhibitors for five days and then immunoblotted (**e**) or stained between two and three weeks later (**f**). **g**, **h**, 451Lu^{BR} cells ablated for the indicated genes were cultured with or without dabrafenib and photographed (**g**) or immunoblotted (**h**) three days later. **i**, Tumours from Fig. 2k were immunostained 18 days after drug discontinuation. Scale bar, 50 μ m. For gel source images, see Supplementary Fig. 1. Data in **c**, **e–h** are representative of three independent biological experiments.

By contrast, although cJUN can mediate a melanoma phenotype switch upon BRAF inhibition and cytokine treatment^{17,18}, it was not strongly or consistently induced by drug removal (Fig. 3c); its ablation failed to prevent cell death induced by drug withdrawal (Extended Data Fig. 5c, d). Upon drug withdrawal, cells became highly migratory, which is another key feature of EMT (Extended Data Fig. 5e, f). Finally, the phenotype switch was not seen in cells that were not drug-addicted (Extended Data Fig. 6a, b).

To investigate whether this phenotype switch could be recapitulated in a clinical setting, we performed immunohistochemical analysis on a set of tumour biopsies from patients with melanoma who had experienced BRAFi relapse. This cohort of biopsies comprised tumours from patients who were still on BRAFi treatment at the time of the biopsy, as well as patients who had already been taken off the drug. We observed that in a highly significant number of cases, treatment discontinuation was correlated with increased AXL expression (Fig. 3d), indicating that at least some features of EMT or phenotype switching can also be observed in a clinical setting.

To examine a potential contribution of MITF to the phenotype switch, we restored its expression by introducing an MITF cDNA into drug-addicted 451Lu^{BR} and A101D^{BMR} cells (Fig. 3e). MITF was at least partially functional, as judged by the attenuation of Melan-A downregulation on drug washout. Restoring MITF substantially protected cells from death by drug withdrawal (Fig. 3f), demonstrating that drug addiction is accompanied by an MITF-dependent phenotype switch, which underlies the associated loss of fitness.

To determine whether the screen hits were functionally connected to phenotype switching, we generated pools of ERK2 and JUNB knockout cells and performed RNA sequencing before and after drug withdrawal. This revealed a shift in transcriptional patterns, notably phenotype switch genes, in control cells that was diminished in the ERK2 knockout derivatives and, to a lesser extent, in the JUNB knockout cells (Extended Data Fig. 7a, b). The prevention of drug washout-induced cell death by means of ERK2 or JUNB depletion was strongly correlated

with maintenance of the MITF signature, and a lack of AP-1, TEAD and JUNB signatures (Extended Data Fig. 7c). As a consequence, the phenotypic changes in cell morphology after drug withdrawal were neutralized in the ERK2 and JUNB knockout cell lines, but not in ERK1 knockout cells (Fig. 3g).

To investigate whether ERK2 is a master regulator of this phenotype switch, we analysed the expression of several proteins associated with this process. Following the loss of ERK2, MITF and its downstream targets BCL-2 and Melan-A were no longer downregulated after drug removal (Fig. 3h). Furthermore, the induction of JUNB and FRA1 after drug withdrawal was diminished in ERK2 knockout cells (but not in ERK1 knockout cells). The ablation of JUNB, too, prevented the decline in MITF after drug withdrawal, but did not affect ERK levels or activity; this suggests that JUNB acts downstream of ERK and upstream of MITF. As judged by their expression of fibronectin and E-cadherin, cells that lacked ERK2 or JUNB, but not ERK1, failed to undergo EMT-like changes following drug withdrawal. In addition, pharmacological inhibition of ERK neutralized the changes in gene expression (Extended Data Fig. 8a) and cell morphology (Extended Data Fig. 8b) that were otherwise observed after drug withdrawal.

We corroborated these *in vitro* observations with *in vivo* experiments. Established control A375^{BR} tumours (Fig. 2k) were largely negative for MITF and its targets, Melan-A and glycoprotein 100 (GP100), after drug discontinuation. By contrast, JUNB or ERK2 knockout melanomas retained their expression of MITF and its targets (Fig. 3i). These results demonstrate that ERK2 and JUNB act in an MITF-dependent genetic phenotype switching programme that governs drug addiction.

Increasing ERK1 and ERK1 phosphorylation to similar levels to those seen for ERK2 after drug removal failed to cause cell death in the absence of ERK2. This suggests that ERK2 functions distinctly from ERK1 in the context of drug addiction (Extended Data Fig. 9a, b) and is consistent with their separate activities in EMT¹⁹. In addition to acquired resistance, tumour cells with enforced BRAFi resistance (by ectopic expression of mutant MEK1^{T55delinsRT}; ref. 20) also experienced declines in viability, and in levels of MITF and its targets, after drug withdrawal (Extended Data Fig. 8c, d).

Because acquired resistance to precision drugs is common across a range of tumour types and drugs, we investigated whether the drug addiction mechanism identified here was also operational in lung cancer. After drug withdrawal, HCC827 cells that were both refractory and addicted to the epidermal growth factor receptor (EGFR) inhibitor CL-387785 experienced a loss of fitness¹ (Fig. 4a). As with melanoma cells, pharmacological (Extended Data Fig. 8e) or genetic ablation of ERK2 (but not ERK1) reversed the drug addiction of these non-small cell lung cancer cells (Fig. 4a, b). Several events preceded this loss of fitness caused by drug withdrawal, including hyperactivation of ERK and MEK, and an EMT/phenotype switch-like reprogramming (Fig. 4c); these were also observed for melanoma cells. We conclude that the ERK2–JUNB–FRA1 pathway responsible for drug addiction in melanoma cells is not limited to a particular tumour or treatment setting.

The extent of lethality imposed by drug addiction can be near total, and produced the very low background of clones in the control arm of our screen (Fig. 1b). Over time, however, clones that were resistant to drug withdrawal spontaneously arose from cell pools (Extended Data Fig. 10a). Functional and biochemical analyses (Extended Data Fig. 10b, c) revealed that they had regained responsiveness to MAPK pathway inhibition. This is consistent with the fact that clinical rechallenges with inhibitors targeting the MAPK pathway in patients whose cancer has progressed on treatment are sometimes successful^{21,22}.

In clinical settings, the emergence of cells that are resistant to drug withdrawal could prevent lasting clinical responses. Therefore, we considered whether combining the cessation of BRAF inhibition with the initiation of another treatment could enhance the durability of these responses. In the past decade, the chemotherapeutic agent dacarbazine (known by the brand name DTIC), an anticancer alkylating agent,

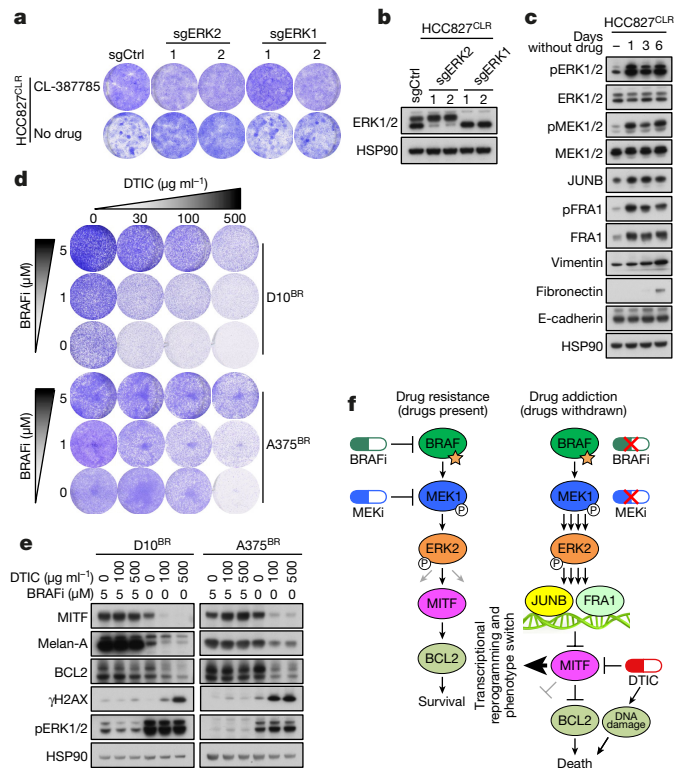


Figure 4 | Conservation of drug addiction mechanism in human lung cancer cells, and drug withdrawal synergizing with dacarbazine in tumour cell elimination. **a, b**, HCC827^{CLR} lung cancer cells ablated for the indicated genes were cultured with or without EGFR tyrosine kinase inhibitor (TKI) CL-387785 and stained 14 days later (**a**) or immunoblotted (**b**). **c**, HCC827^{CLR} cells were cultured with or without CL-387785 for the indicated amount of time and immunoblotted. **d, e**, Moderately drug-addicted D10^{BR} and A375^{BR} melanoma cells were cultured in the presence of the indicated concentrations of dabrafenib and dacarbazine and stained ten days later (**d**) or immunoblotted (**e**). For gel source images, see Supplementary Fig. 1. Data in **a–e** are representative of three independent biological experiments. **f**, Model for the ERK2-dependent phenotype switch that drives cancer drug addiction, in the context of drug pressure and resistance (left), and drug withdrawal causing addiction-associated lethality, irrespective of drug resistance mechanism (right). Grey symbols indicate other potential signalling pathways involved in drug resistance and drug addiction.

has been commonly used as a single agent for metastatic melanoma, albeit with poor response rates²³. We sought to determine whether dacarbazine treatment acts cooperatively with a discontinuation of treatment with BRAFi, and whether it could therefore be used in an alternating therapy strategy. Dacarbazine concentrations of up to 500 $\mu\text{g ml}^{-1}$ had little cytotoxic effect on two drug-resistant and moderately drug-addicted melanoma cell lines in the presence of BRAFi (Fig. 4d). By contrast, when dacarbazine was administered after the BRAFi had been withdrawn, the cytotoxic effects were greatly increased. This was accompanied by the synergistic induction of γH2AX , a marker of double-stranded DNA damage (Fig. 4e) and a cooperative suppression of MITF and its targets Melan-A and BCL-2 (Fig. 4e). The reduction in the levels of the BCL-2 prosurvival protein, combined with the induction of DNA damage, provides a plausible mechanism for the observed synergy between BRAFi withdrawal and dacarbazine treatment in inducing cell death.

Alternating or intermittent therapeutic strategies may create larger therapeutic windows^{21,24–26} than do continuous treatments with single agents. Because clones that have acquired resistance to drug withdrawal can emerge after a long drug ‘holiday’, we suggest that rather than simply halting drug treatments for a set period, therapeutic strategies should

explore optimal alternating treatment modalities. Our results suggest that by developing a more detailed understanding of the molecular mechanism of drug addiction (which seems to be conserved among different tumour types and targeted agents), we may be able to design alternating treatment strategies that enhance mortality among drug-resistant cells after drug withdrawal, producing more durable clinical benefits.

Online Content Methods, along with any additional Extended Data display items and Source Data, are available in the online version of the paper; references unique to these sections appear only in the online paper.

Received 16 February; accepted 25 August 2017.

Published online 4 October 2017.

- Suda, K. *et al.* Conversion from the “oncogene addiction” to “drug addiction” by intensive inhibition of the EGFR and MET in lung cancer with activating EGFR mutation. *Lung Cancer* **76**, 292–299 (2012).
- Sun, C. *et al.* Reversible and adaptive resistance to BRAF(V600E) inhibition in melanoma. *Nature* **508**, 118–122 (2014).
- Moriceau, G. *et al.* Tunable-combinatorial mechanisms of acquired resistance limit the efficacy of BRAF/MEK cotargeting but result in melanoma drug addiction. *Cancer Cell* **27**, 240–256 (2015).
- Thakur, M. D. *et al.* Modelling vemurafenib resistance in melanoma reveals a strategy to forestall drug resistance. *Nature* **494**, 251–255 (2013).
- Seifert, H. *et al.* Prognostic markers and tumour growth kinetics in melanoma patients progressing on vemurafenib. *Melanoma Res.* **26**, 138–144 (2016).
- Dietrich, S. *et al.* Continued response off treatment after BRAF inhibition in refractory hairy cell leukemia. *J. Clin. Oncol.* **31**, e300–e303 (2013).
- Dooley, A. J., Gupta, A. & Middleton, M. R. Ongoing response in BRAF V600E-mutant melanoma after cessation of intermittent vemurafenib therapy: a case report. *Target. Oncol.* **11**, 557–563 (2016).
- Shalem, O. *et al.* Genome-scale CRISPR–Cas9 knockout screening in human cells. *Science* **343**, 84–87 (2014).
- Kemper, K. *et al.* BRAF(V600E) kinase domain duplication identified in therapy-refractory melanoma patient-derived xenografts. *Cell Rep.* **16**, 263–277 (2016).
- Hoek, K. S. & Goding, C. R. Cancer stem cells versus phenotype-switching in melanoma. *Pigment Cell Melanoma Res.* **23**, 746–759 (2010).
- Hoek, K. S. *et al.* *In vivo* switching of human melanoma cells between proliferative and invasive states. *Cancer Res.* **68**, 650–656 (2008).
- Wellbrock, C. & Arozarena, I. Microphthalmia-associated transcription factor in melanoma development and MAP-kinase pathway targeted therapy. *Pigment Cell Melanoma Res.* **28**, 390–406 (2015).
- Garraway, L. A. *et al.* Integrative genomic analyses identify MITF as a lineage survival oncogene amplified in malignant melanoma. *Nature* **436**, 117–122 (2005).
- Verfaillie, A. *et al.* Decoding the regulatory landscape of melanoma reveals TEADS as regulators of the invasive cell state. *Nat. Commun.* **6**, 6683 (2015).
- Konieczkowski, D. J. *et al.* A melanoma cell state distinction influences sensitivity to MAPK pathway inhibitors. *Cancer Discov.* **4**, 816–827 (2014).
- Müller, J. *et al.* Low MITF/AXL ratio predicts early resistance to multiple targeted drugs in melanoma. *Nat. Commun.* **5**, 5712 (2014).
- Ramsdale, R. *et al.* The transcription cofactor c-JUN mediates phenotype switching and BRAF inhibitor resistance in melanoma. *Sci. Signal.* **8**, ra82 (2015).
- Riesenberg, S. *et al.* MITF and c-Jun antagonism interconnects melanoma dedifferentiation with pro-inflammatory cytokine responsiveness and myeloid cell recruitment. *Nat. Commun.* **6**, 8755 (2015).
- Shin, S., Dimitri, C. A., Yoon, S.-O., Dowdle, W. & Blenis, J. ERK2 but not ERK1 induces epithelial-to-mesenchymal transformation via DEF motif-dependent signaling events. *Mol. Cell* **38**, 114–127 (2010).
- Kemper, K. *et al.* Intra- and inter-tumor heterogeneity in a vemurafenib-resistant melanoma patient and derived xenografts. *EMBO Mol. Med.* **7**, 1104–1118 (2015).
- Seghers, A. C., Wilgenhof, S., Lebbé, C. & Neyns, B. Successful rechallenge in two patients with BRAF-V600-mutant melanoma who experienced previous progression during treatment with a selective BRAF inhibitor. *Melanoma Res.* **22**, 466–472 (2012).
- Schreuer, M. *et al.* Combination of dabrafenib plus trametinib for BRAF and MEK inhibitor pretreated patients with advanced BRAF(V600)-mutant melanoma: an open-label, single arm, dual-centre, phase 2 clinical trial. *Lancet Oncol.* **18**, 464–472 (2017).
- Harries, M. *et al.* Treatment patterns of advanced malignant melanoma (stage III-IV) - A review of current standards in Europe. *Eur. J. Cancer* **60**, 179–189 (2016).
- Jain, T. & Bryce, A. Intermittent BRAF inhibition can achieve prolonged disease control in BRAF mutant melanoma. *Cureus* **7**, e410 (2015).
- Abdel-Wahab, O. *et al.* Efficacy of intermittent combined RAF and MEK inhibition in a patient with concurrent BRAF- and NRAS-mutant malignancies. *Cancer Discov.* **4**, 538–545 (2014).
- Dooley, A. J., Gupta, A., Bhattacharyya, M. & Middleton, M. R. Intermittent dosing with vemurafenib in BRAF V600E-mutant melanoma: review of a case series. *Ther. Adv. Med. Oncol.* **6**, 262–266 (2014).

Supplementary Information is available in the online version of the paper.

Acknowledgements We are grateful to K. Suda and T. Mitsudomi for HCC827 and HCC827^{CLR} cells, J. Villanueva for 451Lu cells, I. de Krijger for technical advice on FISH, A. Broeks and the NKI Biobank for help with patient samples, R. Beijersbergen for providing the GeCKO library and A. Huitema for providing DTIC. We thank all members of the Peeper and Blank labs for advice. This work was financially supported by the European Research Council under the European Union’s Seventh Framework Programme (FP7/2007–2013) /ERC synergy grant agreement number 319661 COMBATCANCER (X.K., D.S.P.), and a Fellowship (T.K.), a Queen Wilhelmina Award (D.S.P.) and a research grant (nr. 10304; X.K., D.S.P.), all by the Dutch Cancer Society/Koningin Wilhelmina Fonds.

Author Contributions X.K., T.K. and D.S.P. designed all experiments. All *in vitro* experiments were carried out by X.K., with the exception of a reverse transcription PCR analysis done by K.K. Xenograft experiments were done by A.S. T.K. performed all bioinformatic analyses. J.-Y.S. analysed mouse tumours. J.B., E.A.R., M.H.G.F. and H.W.M.N. analysed human melanoma samples in collaboration with C.U.B. X.K. and D.S.P. wrote the manuscript. All authors revised and approved the manuscript. The project was supervised by D.S.P.

Author Information Reprints and permissions information is available at www.nature.com/reprints. The authors declare no competing financial interests. Readers are welcome to comment on the online version of the paper. Publisher’s note: Springer Nature remains neutral with regard to jurisdictional claims in published maps and institutional affiliations. Correspondence and requests for materials should be addressed to D.S.P. (d.peeper@nki.nl).

Reviewer Information *Nature* thanks R. Marais, D. Solit and the other anonymous reviewer(s) for their contribution to the peer review of this work.

METHODS

No statistical methods were used to predetermine sample size. Unless otherwise stated, the experiments were not randomized and the investigators were not blinded to allocation during experiments and outcome assessment.

GeCKO screen. Drug-addicted 451Lu^{BR} cells were lentivirally transduced with two GeCKO libraries (A and B)⁸. Two days after infection, cells were selected with puromycin (2 µg ml⁻¹) for three days. Cells were split into two pools; one was subjected to BRAFi dabrafenib (1 µM) treatment, and the other was left untreated. Cell colonies that formed in the drug-deprived group were individually picked and expanded. For identification of sgRNAs in individual clones, genomic DNA was isolated and sgRNAs were recovered by PCR amplification. Amplified DNA fragments were cloned into the TOPO TA-cloning vector (450071, Invitrogen), and the sgRNA was identified using Sanger sequencing.

Compounds. The BRAF inhibitors dabrafenib and PLX4720, the MEK inhibitor trametinib, the ERK inhibitor SCH727284 and the EGFR TKI CL-387785 were purchased from Selleck Chemicals. Dacarbazine was obtained from the pharmacy of the Slotervaart hospital.

Cell lines. A375, Mel888, A101D, SK-Mel-28, D10 and HEK293T cells were from the Peeper laboratory cell line stock. HCC827 and HCC827^{CLR} cells were from K. Suda and T. Mitsudomi (Kindai University) and 451Lu cells from J. Villanueva (The Wistar Institute). All cell lines were authenticated by STR profiling (Promega) and routinely tested for mycoplasma contamination. All cell lines were cultured in DMEM supplemented with 9% fetal bovine serum (Sigma), plus 100 units per ml penicillin and 0.1 mg ml⁻¹ streptomycin (Gibco). To generate BRAFi or BRAFi + MEKi-resistant cells, parental drug-sensitive cells were exposed to increasing concentrations of BRAFi dabrafenib (from 0.01 µM to 5 µM) or BRAFi dabrafenib + MEKi trametinib (from 0.01 µM + 0.001 µM to 0.5 µM + 0.05 µM) for 3–5 months. PLX4720-resistant cells were generated as previously described¹⁶. The resistance was confirmed by measuring cell viability under drug treatment.

Colony formation assay. Colony formation assays were performed in 12-well plates by seeding 3,000 cells (A101D^{BMR}), 10,000 cells (HCC827^{CLR}, SK-Mel-28^{BR}, Mel888^{PLXR}, A375^{PLXR}, A375^{WR}, 451Lu^{WR}, A101D^{WR} and all parental drug-sensitive cells), 30,000 cells (Mel888^{BMR}), or 50,000 cells (451Lu^{BR}, A375^{BMR}, A375^{BR}, D10^{BR} and D10^{BMR}). Medium was refreshed twice per week and plates were fixed in 4% formaldehyde solution, stained with crystal violet (1% in 50% methanol) and photographed after 10–21 days of treatment (as indicated).

Animal studies. Animal work procedures were approved by the animal experimental committee of the NKI and performed according to Dutch law. The *in vivo* experiment was performed with A375^{BMR} cells infected with lentivirus encoding sgRNAs. Cells (10⁶) were injected subcutaneously into both flanks of 5–7-week-old female NSG mice. The mice received dabrafenib and trametinib by daily oral gavage, from the first day of tumour injection until drug treatment was stopped. Tumour growth rates were analysed by measuring tumour length (*L*) and width (*W*), and calculating volume through the use of the formula $LW^2/2$.

Human melanoma specimens. Patient melanoma samples were obtained (following Institutional Review Board approval) from the NKI-AVL pathology archive biobank. Informed consent was obtained from all patients.

Immunohistochemistry and scoring. AXL staining was performed manually. After deparaffinization of FFPE-fixed slides using xylene, antigen retrieval was performed using citrate buffer (pH 6) in a pressure cooker for 5 min. Sections were treated with 0.3% H₂O₂ to block endogenous peroxidase activity and subsequently blocked in 10% human serum in PBS-T for 30 min. Primary AXL antibody (sc-20741, Santa Cruz) was applied at a concentration of 3 µg ml⁻¹ for 1 hour at room temperature. Detection was performed with an anti-rabbit HRP-conjugated antibody (Immunologic, Brightvision) and developed using AEC and a counterstain of haematoxylin. Slides were manually analysed by a certified pathologist from the VU Medical Center in a blinded fashion. The percentage of AXL positive cells was determined by analysing whole slides of every sample. MITF (clone C5/D5, Immunologic), Melan-A and GP100 (ab732, Abcam) stainings in mouse xenograft tumours were performed using the protocol described above, with minor modifications (they were blocked with goat serum, incubated with anti-mouse HRP-conjugated antibody and developed with DAB).

Immunoblotting. Immunoblotting was performed as previously described¹⁶. The following antibodies were used: pERK1/2 (Thr202/Tyr204, 9106), ERK1/2 (9102), pMEK1/2 (Ser217/221, 9154), MEK1/2 (4694), MEK1 (2352), MEK2 (9147), JUNB (3753), pFRA1 (Ser265, 5841), p-cJUN (Ser73, 3270) and cJUN (2315) BCL-2 (4223) from Cell Signaling Technology; BRAF^{V600E} (E19290) from Spring

Bioscience; ATK (sc-8312), pAKT (Ser473, sc-7985-R), FRA1 (sc-28310), BRAF (sc-5284), BCL-2 (sc-492) and HSP90 (sc-7947) from Santa Cruz Biotechnology; MITF (ab12039) and AXL (ab89224) from Abcam; Melan-A (M7196) from Dako; E-cadherin (610181), Vimentin (550513) and Fibronectin (610077) from BD Bioscience. The antibodies were diluted according to manufacturers' instructions.

Fluorescence *in situ* hybridization. Preparation of metaphase chromosome spreads from A375 and A375^{BMR} cells was performed as previously described²⁷. Two-colour metaphase FISH was performed using a *BRAF* probe (7q34 BRAF-CN RD, G100368R-8, Agilent) and a probe located on the chromosome 7 centromere (Chr7 CEP GR, G100527G-8, Agilent), according to the manufacturer's protocol.

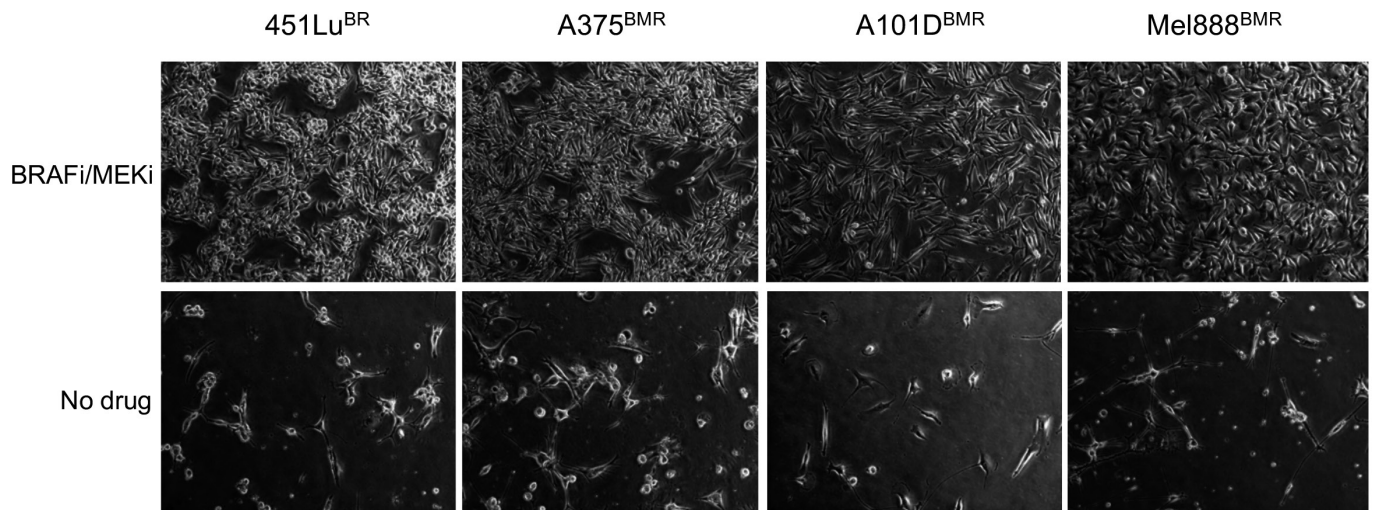
PCR, Sanger sequencing, cloning and lentivirus production. All primer sequences are listed in Supplementary Table 2. For identification of *BRAF* amplification in A375^{BMR} cell, genomic DNA was isolated and quantitative PCR was performed with primers amplifying *BRAF*, *CRAF* and *LINE*. For identification of the *MAP2K1* mutation in 451Lu^{BR} cells, genomic DNA was isolated and *MAP2K1* exon 2 was cloned into the TOPO TA-cloning vector (450071, Invitrogen), followed by Sanger sequencing. The presence of BRAF^{V600E/DK} in Mel888^{BMR} cells was identified as previously described⁹. For construction of an sgRNA-expressing vector, DNA oligonucleotides (Invitrogen) were annealed and ligated into BsmBI-digested LentiCRISPRv2 plasmid. Target sgRNA oligonucleotide sequences are listed in Supplementary Table 2. The plasmid encoding the MITF-M isoform has been previously described¹⁶. Production of lentivirus was performed as previously described²⁸.

Transwell migration assay. To examine the migration potential, cells were cultured in the presence or absence of MAPK pathway inhibitors for 1 day followed by seeding 200,000 cells into the top chambers of a transwell (3422, Corning) in serum-free medium, with or without inhibitors. The lower compartment contained medium supplemented with 9% fetal bovine serum as a chemoattractant. Cells were incubated for 8 (A101D^{BMR}) or 24 (451Lu^{BR}) hours and cells that did not migrate through the pores were removed with a cotton swab. Filters were fixed in 4% formaldehyde solution, stained with 0.1% crystal violet and photographed, and then cells were counted.

RNA sequencing analysis. RNA was isolated using Trizol, and cDNA libraries were sequenced on an Illumina HiSeq2000 to obtain 65-bp single-end sequence reads. Reads were aligned to the GRCh38 human reference genome using TopHat (2.1.0), and gene counts were obtained using HTSeq-count. All downstream analyses were performed in R using the Bioconductor framework. DESeq2 rlog-values were used for visualization of gene expression levels in heat maps. Heat maps represent mean rlog-values of two independent biological replicate experiments. Clustering was performed using the default settings of the heatmap.2 function in the gplots package. For Extended Data Fig. 5a, gene-wise scaling was applied to rlog-values; the 200 most variable values are represented. For Fig. 3a and Extended Data Fig. 7a, b, rlog-values were mean normalized on a gene-wise basis. For GSEAs, counts per million were used as input. For Fig. 3b and Extended Data Fig. 5b, time points were converted to a ranking score (0, 1, 2 and 3 for time points 0, 6, 24 and 48 hours of A375^{BMR} or 0, 1, 3 and 5 days of 451Lu^{BR}, respectively). For Extended Data Fig. 7c, the extent of rescue from cell death was converted to a ranking score (1, 2, 3, or 4 for Mel888^{BMR} cells expressing sgCtrl, sgJUNB, or sgERK2 in the context of drug removal, and Mel888^{BMR} cells with treatment, respectively). Pre-ranked gene lists were created by correlating these ranking scores with gene expression using the Spearman's rank correlation coefficient metric. Phenotype switching and MITF target gene lists were obtained from http://www.jurmo.ch/work_mitf.php. The TEAD and AP1 signatures were taken from ref. 14, and the JUNB signature was derived from supplementary table 3a of ref. 29, where human homologues of mouse genes were derived using the biomaRt package. Analyses were performed using javaGSEA³⁰ and replotted from the output of this tool using the replotGSEA function (<https://github.com/PeeperLab/Rtoolbox>).

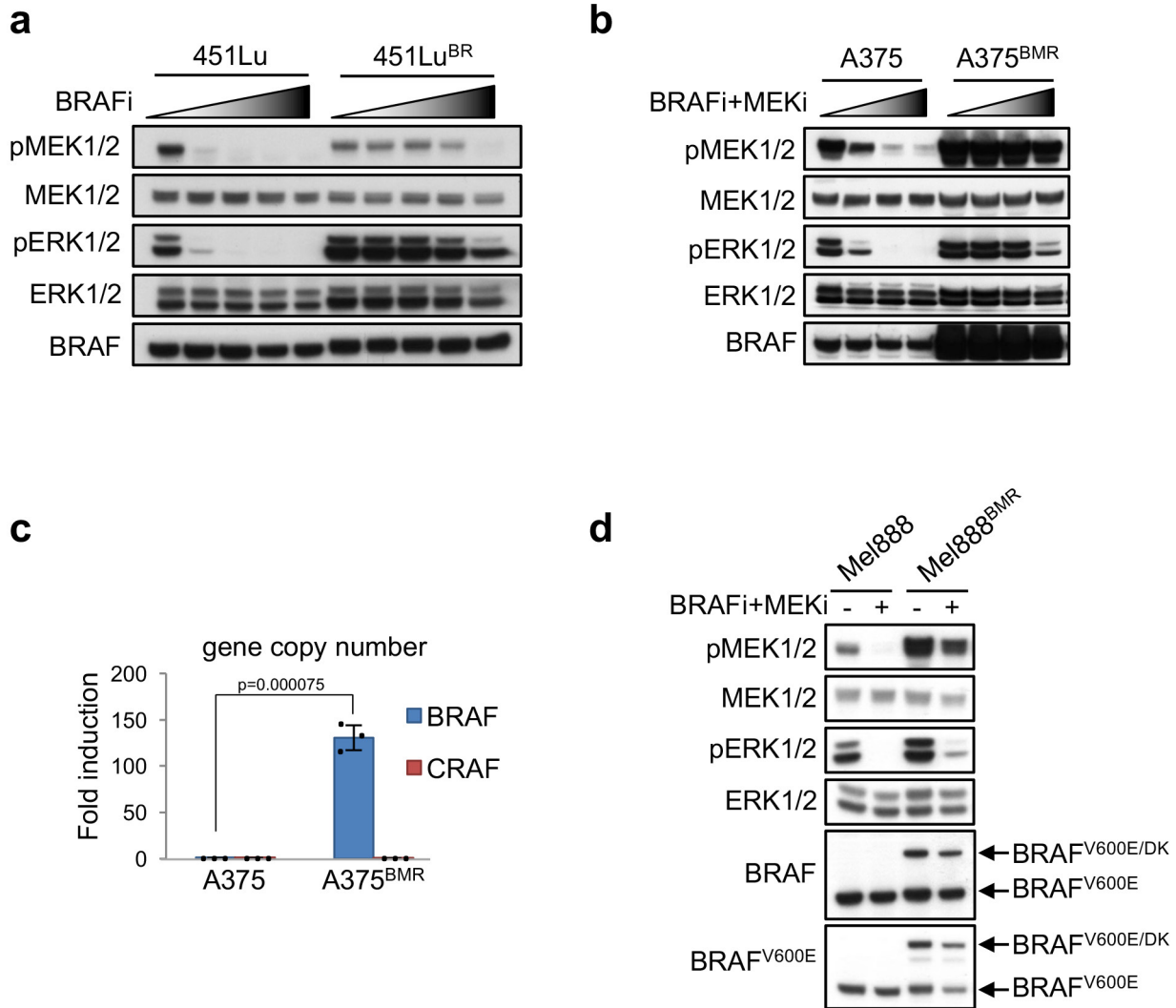
Data availability. All sequencing datasets have been deposited in the NCBI Gene Expression Omnibus under accession numbers GSE98866 and GSE98867.

- van Steensel, B., Smogorzewska, A. & de Lange, T. TRF2 protects human telomeres from end-to-end fusions. *Cell* **92**, 401–413 (1998).
- Vredevel, L. C. W. *et al.* Abrogation of BRAF^{V600E}-induced senescence by PI3K pathway activation contributes to melanomagenesis. *Genes Dev.* **26**, 1055–1069 (2012).
- Fontana, M. F. *et al.* JUNB is a key transcriptional modulator of macrophage activation. *J. Immunol.* **194**, 177–186 (2015).
- Subramanian, A. *et al.* Gene set enrichment analysis: a knowledge-based approach for interpreting genome-wide expression profiles. *Proc. Natl Acad. Sci. USA* **102**, 15545–15550 (2005).



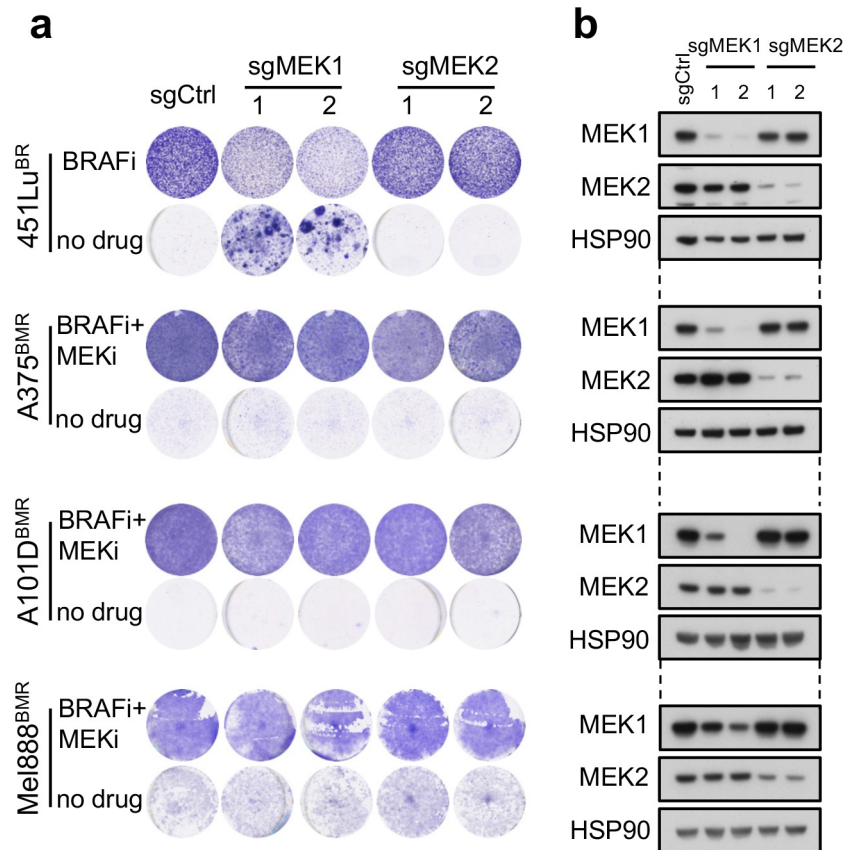
Extended Data Figure 1 | Drug addiction phenotype in acquired-drug-resistant melanoma cells. Acquired BRAFi-resistant 451Lu^{BR} cells were cultured in the presence or absence of 1 μ M BRAFi; acquired BRAFi + MEKi-resistant A375^{BMR}, A101D^{BMR} and Mel888^{BMR} cells were

cultured in the presence or absence of 0.5 μ M BRAFi + 0.05 μ M MEKi. Photographs were taken after seven days. The images are representative of three independent biological experiments.



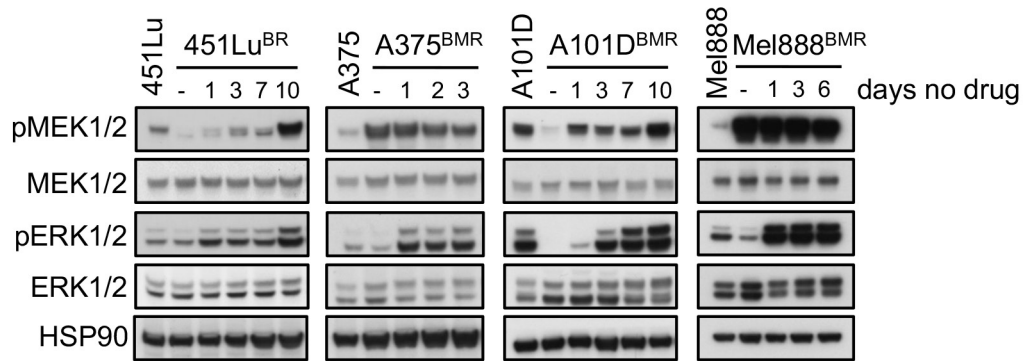
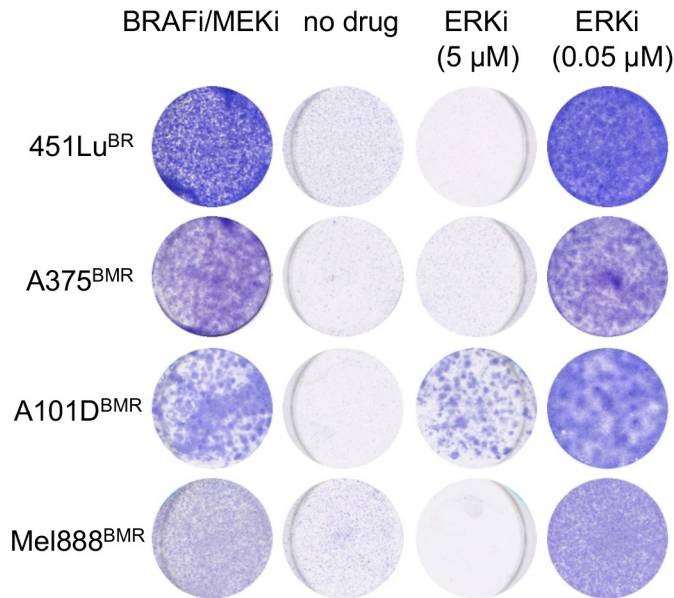
Extended Data Figure 2 | Generation of a diverse melanoma cell line panel with distinct drug resistance mechanisms. **a**, 451Lu and 451Lu^{BR} cells were treated with increasing concentrations of dabrafenib (0, 0.01, 0.1, 1 and 10 μ M) for six hours. Total cell lysates were subjected to immunoblotting with indicated antibodies. ERK1/2 served as a loading control. **b**, A375 and A375^{BMR} cells were treated with increasing concentrations of the BRAFi dabrafenib + MEKi trametinib (0 + 0 μ M, 0.01 + 0.001 μ M, 0.1 + 0.01 μ M and 1 + 0.1 μ M) for six hours. Total cell lysates were subjected to immunoblotting with indicated antibodies. ERK1/2 served as a loading control. **c**, Quantification of *BRAF*

amplification by quantitative PCR on genomic DNA of A375 and A375^{BMR} cells. *CRAF* was included as a negative control. Cycle threshold values were normalized to *LINE*. *P* value calculated by unpaired two-sided Student's *t*-test. Data in graphs are mean \pm s.d. from three technical replicates; confidence interval 95%. **d**, Mel888 and Mel888^{BMR} cells were treated with vehicle or 0.5 μ M BRAFi + 0.05 μ M MEKi for six hours. Total cell lysates were subjected to immunoblotting with indicated antibodies. ERK1/2 served as a loading control. For gel source images, see Supplementary Fig. 1. Data in **a–d** are representative of three independent biological experiments.



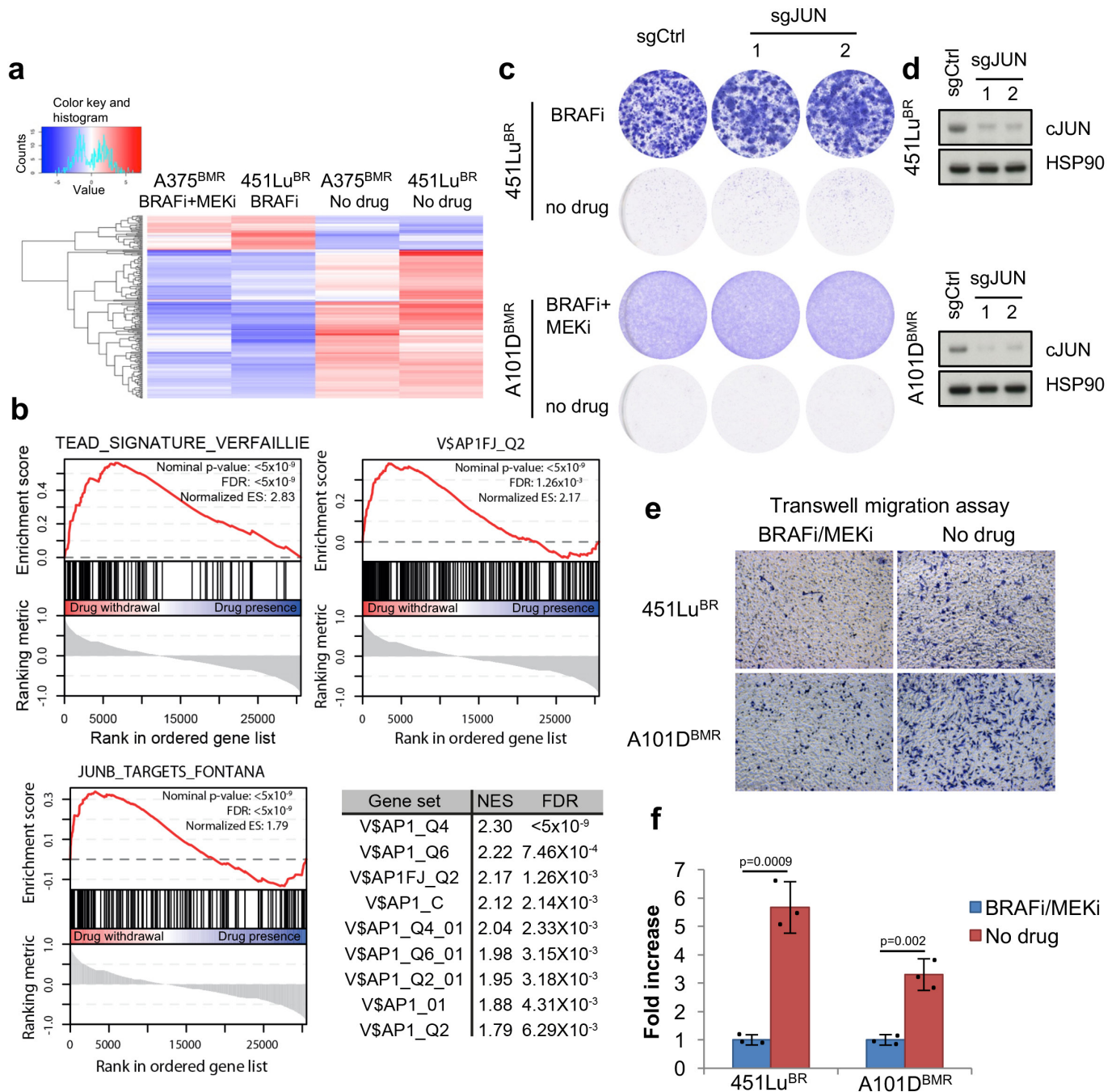
Extended Data Figure 3 | Disruption of MEK1 prevents mortality in drug-addicted 451Lu^{BR} cells after drug withdrawal. **a**, 451Lu^{BR}, A375^{BMR}, A101D^{BMR} and Mel888^{BMR} cells were infected with lentivirus that expressed sgRNAs targeting genes *MAP2K1* (encoding MEK1), *MAP2K2* (encoding MEK2) or a scrambled sequence (sgCtrl). Cells were seeded in the presence or absence of MAPK pathway inhibitors, and

fixed, stained and photographed after 14 days (BRAFi or BRAFi + MEKi group) or 21 days (no drug group). **b**, Cell lysates from **a** were subjected to immunoblotting using the indicated antibodies. HSP90 served as a loading control. For gel source images, see Supplementary Fig. 1. Data in **a** and **b** are representative of three independent biological experiments.

a**b**

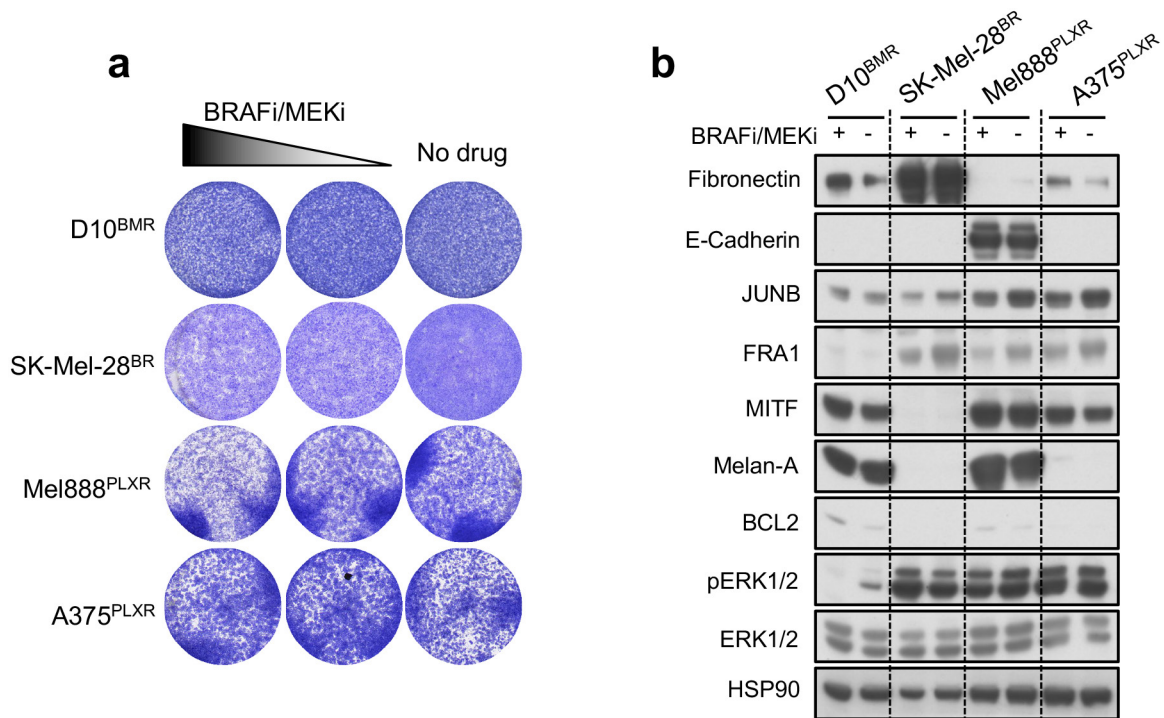
Extended Data Figure 4 | ERK rebound contributes to drug withdrawal lethality irrespective of drug resistance mechanism. **a**, Four parental drug-sensitive cell lines were cultured without MAPK pathway inhibitors, and their drug-resistant counterparts were cultured in the presence or absence of MAPK pathway inhibitors, for the indicated number of days. Total cell lysates were subjected to immunoblotting with indicated antibodies. HSP90 served as a loading control. **b**, 451Lu^{BR} cells were

cultured in the presence of 1 μM BRAFi, a high concentration (5 μM) of ERKi, a low concentration (0.05 μM) of ERKi, or vehicle control (no drug). A375^{BMR}, A101D^{BMR} and Mel888^{BMR} cells were cultured with 0.5 μM BRAFi + 0.05 μM MEKi, 5 μM ERKi, 0.05 μM ERKi or vehicle control (no drug). Cells were fixed, stained and photographed after 14 days. For gel source images, see Supplementary Fig. 1. Data in **a** and **b** are representative of two independent biological experiments.



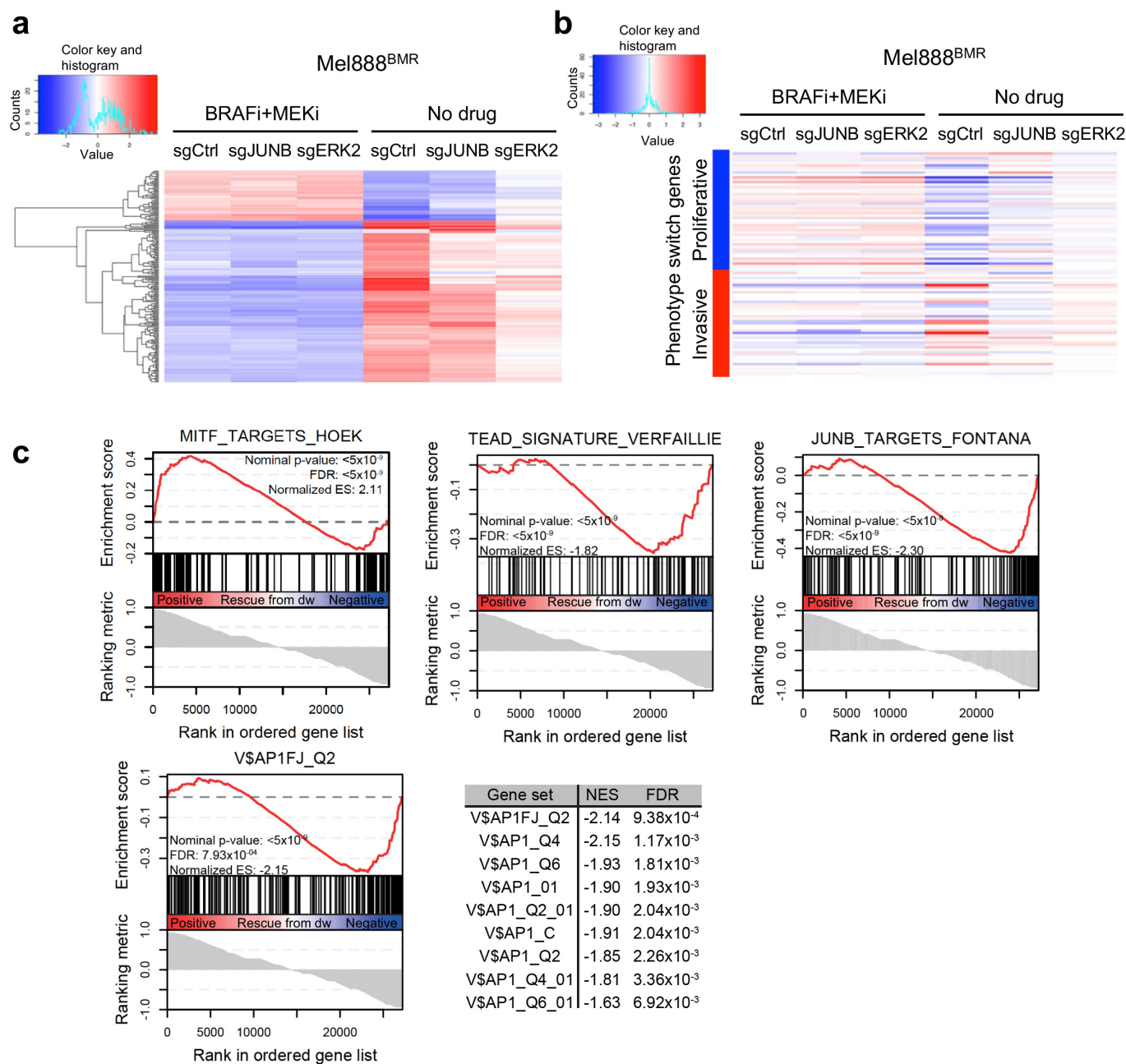
Extended Data Figure 5 | Drug addiction is relayed by an MITF-dependent phenotype switch. **a**, Drug-addicted A375^{BMR} cells were cultured in the absence of 0.5 μ M BRAFi + 0.05 μ M MEKi for 0, 6, 24 and 48 h, and 451Lu^{BR} cells were cultured in the absence of 1 μ M BRAFi for 0, 1, 3 and 5 days. Total RNA was isolated and subjected to sequencing analysis. Unsupervised clustering of the 200 most variably expressed genes is represented for the first (either 0 h or 0 days) and last time points (either 48 h or 5 days) in a heat map. **b**, Sequence data in **a** (all time points) were subjected to GSEA to determine the correlation of the indicated gene sets with the drug addiction effect in A375^{BMR} and 451Lu^{BR} cells. For *P* value calculation, see Methods. **c**, 451Lu^{BR} and A101D^{BMR} cells were infected with lentivirus that expressed sgRNAs targeting gene encoding cJUN (sgJUN) or a scrambled sequence (sgCtrl). Cells were seeded in the

presence or absence of MAPK pathway inhibitors, and fixed, stained and photographed after 14 days (BRAFi or BRAFi + MEKi group) or 21 days (no drug group). **d**, Total cell lysates of the samples in **c** were subjected to immunoblotting analysis with indicated antibodies. HSP90 served as a loading control. **e**, 451Lu^{BR} and A101D^{BMR} cells were cultured in the presence or absence of the MAPK pathway inhibitors for 24 h and then subjected to a transwell migration assay. The cells that migrated through the membrane were fixed, stained and photographed after 8 (A101D^{BMR}) or 24 (451Lu^{BR}) hours. **f**, Quantification of the migration capacity (**e**) from three representative images from each sample; *P* value calculated by unpaired two-sided Student's *t*-test. Data in graphs are mean \pm s.d. For gel source images, see Supplementary Fig. 1. Data in **c–e** are representative of two independent biological experiments.



Extended Data Figure 6 | Phenotype switch is not observed in non drug-addicted cells upon drug withdrawal. **a**, D10^{BMR} cells were cultured with 1 μ M BRAFi + 0.1 μ M MEKi, 0.5 μ M BRAFi + 0.05 μ M MEKi or vehicle control (no drug); SK-Mel-28^{BR} cells were cultured with either 3 μ M BRAFi dabrafenib, 1 μ M dabrafenib or vehicle control (no drug); Mel888^{PLXR} and A375^{PLXR} cells were cultured with 3 μ M BRAFi PLX4720,

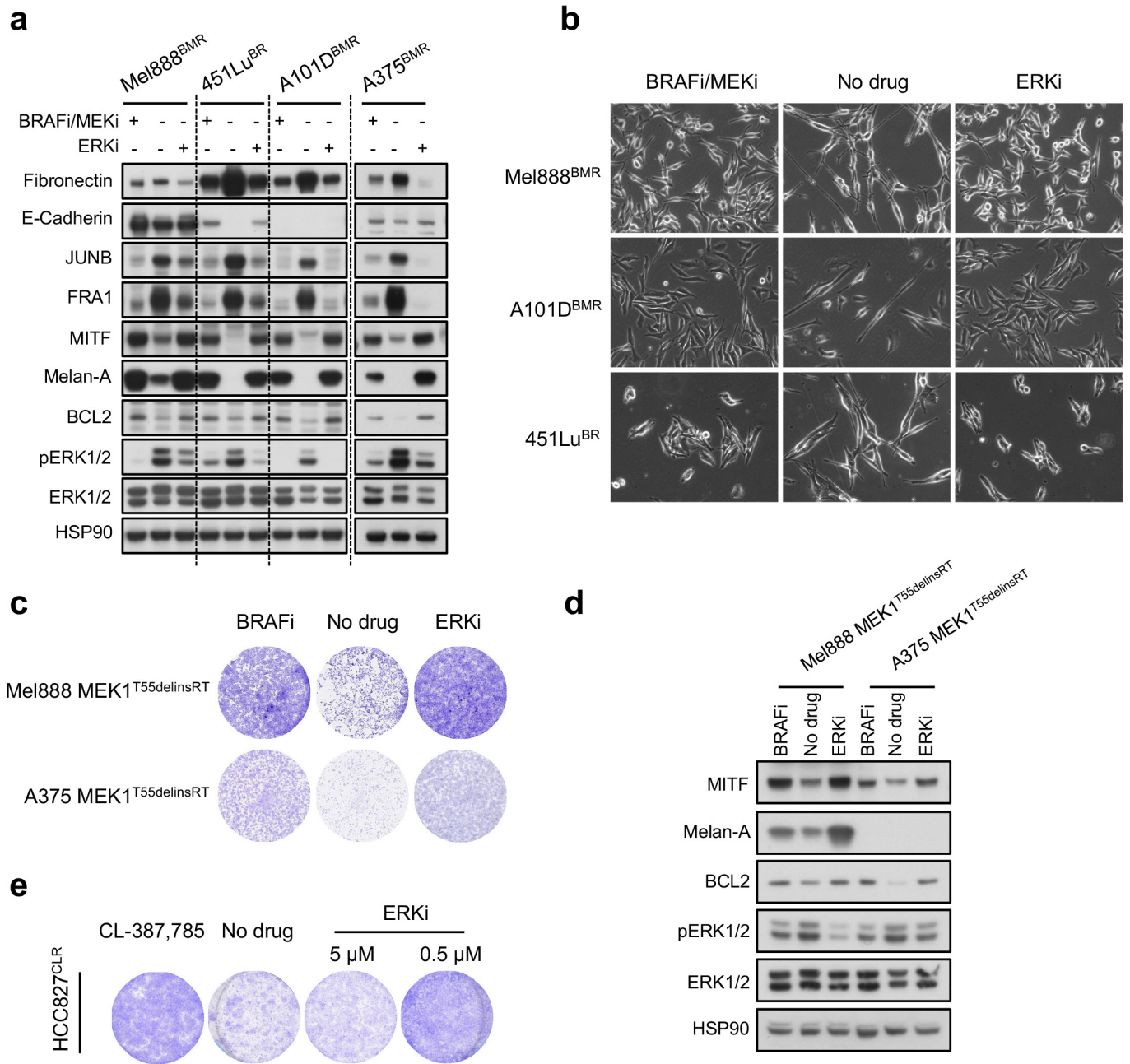
1 μ M PLX4720 or vehicle control (no drug); Cells were fixed, stained and photographed after ten days. **b**, On the third day, total cell lysates of the samples in **a** were subjected to immunoblotting analysis with indicated antibodies. HSP90 served as a loading control. For gel source images, see Supplementary Fig. 1. Data in **a** and **b** are representative of two independent biological experiments.



Extended Data Figure 7 | ERK2 and JUNB act in an MITF-dependent genetic phenotype switching program controlling drug addiction.

a, Mel888^{BMR} cells were infected with lentivirus expressing sgRNAs targeting genes encoding JUNB (sgJUNB), ERK2 (sgERK2) or a scrambled sequence (sgCtrl). Cells were cultured in the presence or absence of 0.5 μ M BRAFi + 0.05 μ M MEKi for five days. Total RNA was isolated and subjected to sequencing analysis. Unsupervised clustering of the 200 most

variably expressed genes is represented in a heat map. **b**, Genes involved in phenotype switching were selected from the sequence data in **a** and are represented in a heat map. **c**, Sequence data in **a** were subjected to GSEA to determine the correlation of the indicated gene sets with the extent of rescue of the drug addiction phenotype by sgJUNB and sgERK2 in Mel888^{BMR} cells. dw, drug withdrawal. For *P* value calculation, see Methods.

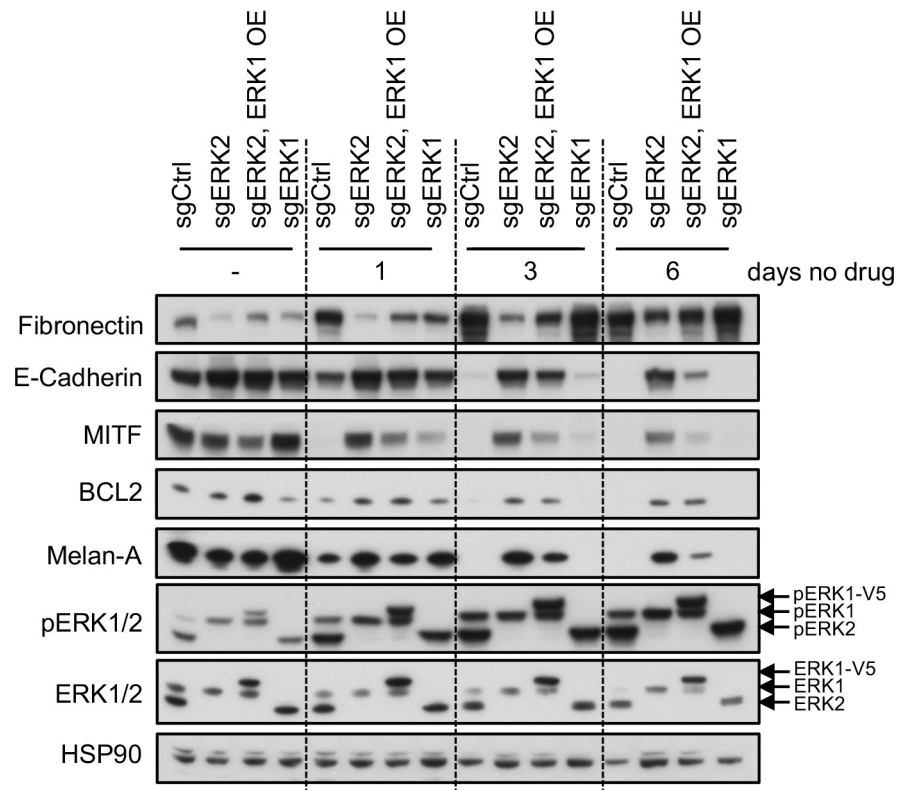


Extended Data Figure 8 | Pharmacological ERK inhibition blocks phenotype switch in drug-addicted cells upon drug withdrawal.

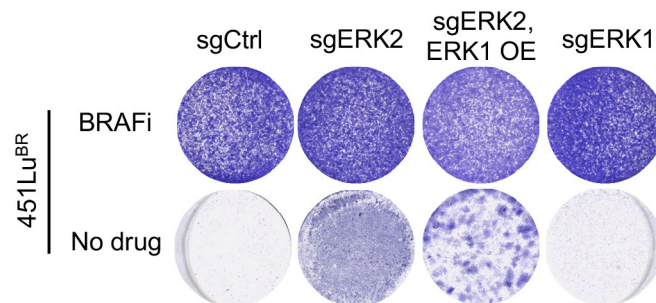
a, Mel888^{BMR}, A101D^{BMR} and A375^{BMR} cells were cultured with 0.5 μM BRAFi + 0.05 μM MEKi, vehicle or 0.05 μM ERKi, 451Lu^{BR} cells were cultured with 1 μM BRAFi, vehicle or 0.05 μM ERKi for three days. Total cell lysates were subjected to immunoblotting with indicated antibodies. HSP90 served as a loading control. **b**, Photographs taken of cells in **a**, on the third day. **c**, Mel888 MEK1^{T55delinsRT} and A375 MEK1^{T55delinsRT} cells were cultured in the presence of 0.3 μM BRAFi, low concentration

(0.05 μM) of ERKi or vehicle control (no drug). Cells were fixed, stained and photographed after ten days. **d**, On the fifth day, total cell lysates from cells in **c** were subjected to immunoblotting with indicated antibodies. HSP90 served as a loading control. **e**, HCC827^{CLR} cells were cultured in the presence of 1 μM EGFR TKI CL-387785, a high concentration (5 μM) of ERKi, a low concentration (0.5 μM) of ERKi, or with vehicle control (no drug). Cells were fixed, stained and photographed after 14 days. For gel source images, see Supplementary Fig. 1. Data in **a–e** are representative of three independent biological experiments.

a

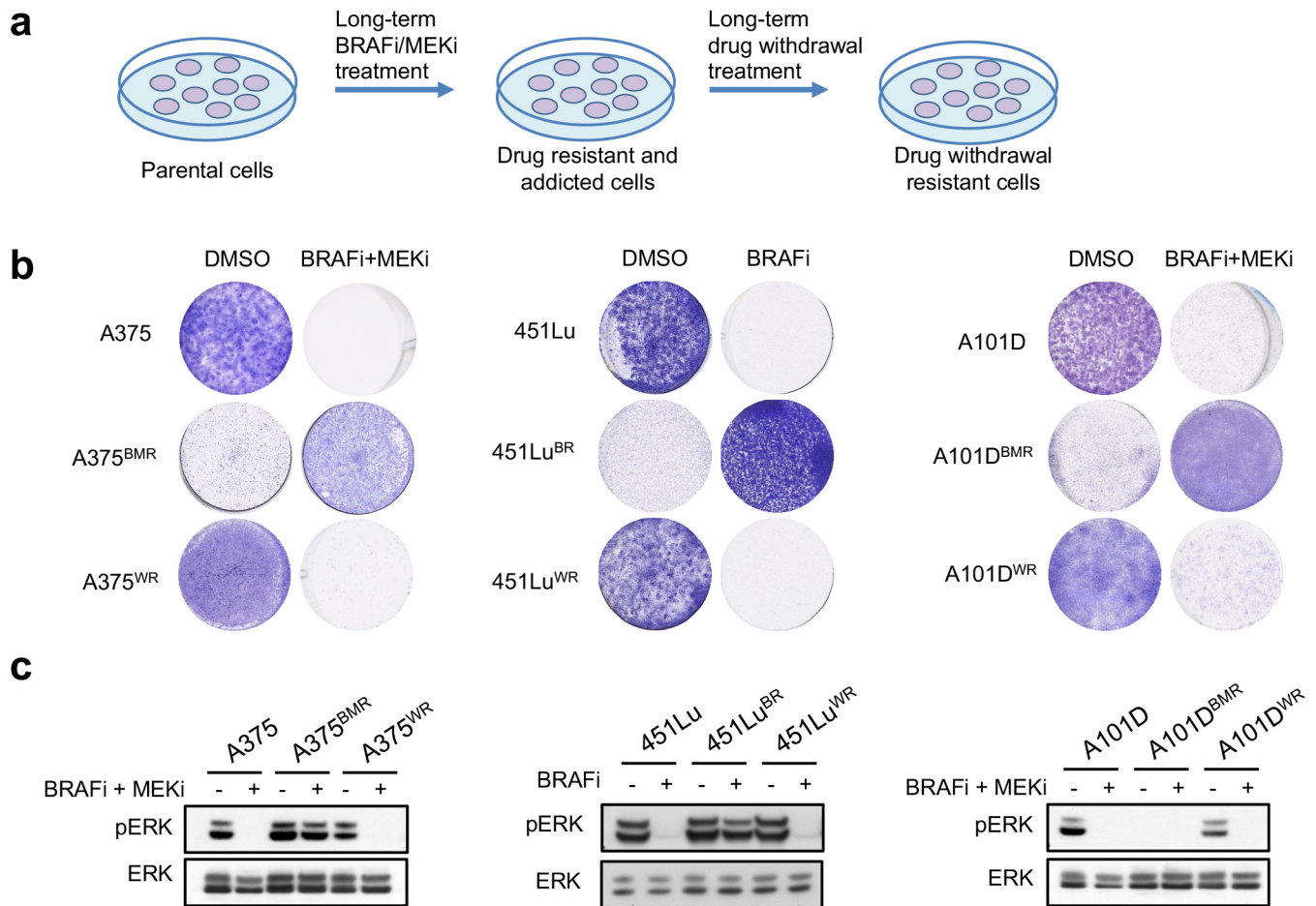


b



Extended Data Figure 9 | ERK2 and ERK1 have distinct functions in drug addiction. **a**, 451Lu^{BR} control cells (sgCtrl), ERK2 knockout cells (sgERK2), ERK1 (v5-tagged)-overexpressing sgERK2 cells (sgERK2, ERK1 OE) and ERK1 knockout cells (sgERK1) were cultured in the presence or absence of 1 μ M BRAFi for up to six days. Total cell lysates were subjected to immunoblotting analysis with indicated antibodies.

HSP90 served as a loading control. **b**, Cells described in **a** were cultured in the presence or absence of BRAFi, and fixed, stained and photographed after 14 days (BRAFi group) or 21 days (no drug group). For gel source images, see Supplementary Fig. 1. Data in **a** and **b** are representative of two independent biological experiments.



Extended Data Figure 10 | Dynamic phenotype of drug resistance and drug addiction in melanoma. **a**, Schematic flow chart indicating drug withdrawal resistant cells were generated from drug-addicted cells with long-term drug withdrawal. **b**, Parental (A375, 451Lu and A101D) cells, acquired-drug-resistant (A375^{BMR}, 451Lu^{BR} and A101D^{BMR}) cells and spontaneously developed drug withdrawal-resistant (A375^{WR}, 451Lu^{WR}

and A101D^{WR}) cells were cultured with MAPK pathway inhibitors or vehicle. Cells were fixed, stained and photographed after 14 days. **c**, Total cell lysates from cells in **b** were subjected to immunoblotting with pERK and ERK antibodies after six hours treatment. For gel source images, see Supplementary Fig. 1. Data in **b** and **c** are representative of three independent biological experiments.

Life Sciences Reporting Summary

Nature Research wishes to improve the reproducibility of the work that we publish. This form is intended for publication with all accepted life science papers and provides structure for consistency and transparency in reporting. Every life science submission will use this form; some list items might not apply to an individual manuscript, but all fields must be completed for clarity.

For further information on the points included in this form, see [Reporting Life Sciences Research](#). For further information on Nature Research policies, including our [data availability policy](#), see [Authors & Referees](#) and the [Editorial Policy Checklist](#).

▶ Experimental design

1. Sample size

Describe how sample size was determined.

Sample size was determined on the basis of essential control samples + the experimental samples.

2. Data exclusions

Describe any data exclusions.

Not applicable.

3. Replication

Describe whether the experimental findings were reliably reproduced.

We have indicated this in the figure legends.

4. Randomization

Describe how samples/organisms/participants were allocated into experimental groups.

There was no reason to randomize experiments for this study.

5. Blinding

Describe whether the investigators were blinded to group allocation during data collection and/or analysis.

Yes, this was done for IHC scoring.

Note: all studies involving animals and/or human research participants must disclose whether blinding and randomization were used.

6. Statistical parameters

For all figures and tables that use statistical methods, confirm that the following items are present in relevant figure legends (or in the Methods section if additional space is needed).

- | | |
|-------------------------------------|--|
| n/a | Confirmed |
| <input type="checkbox"/> | <input checked="" type="checkbox"/> The <u>exact sample size</u> (n) for each experimental group/condition, given as a discrete number and unit of measurement (animals, litters, cultures, etc.) |
| <input type="checkbox"/> | <input checked="" type="checkbox"/> A description of how samples were collected, noting whether measurements were taken from distinct samples or whether the same sample was measured repeatedly |
| <input type="checkbox"/> | <input checked="" type="checkbox"/> A statement indicating how many times each experiment was replicated |
| <input type="checkbox"/> | <input checked="" type="checkbox"/> The statistical test(s) used and whether they are one- or two-sided (note: only common tests should be described solely by name; more complex techniques should be described in the Methods section) |
| <input checked="" type="checkbox"/> | <input type="checkbox"/> A description of any assumptions or corrections, such as an adjustment for multiple comparisons |
| <input type="checkbox"/> | <input checked="" type="checkbox"/> The test results (e.g. P values) given as exact values whenever possible and with confidence intervals noted |
| <input type="checkbox"/> | <input checked="" type="checkbox"/> A clear description of statistics including <u>central tendency</u> (e.g. median, mean) and <u>variation</u> (e.g. standard deviation, interquartile range) |
| <input type="checkbox"/> | <input checked="" type="checkbox"/> Clearly defined error bars |

See the web collection on [statistics for biologists](#) for further resources and guidance.

► Software

Policy information about [availability of computer code](#)

7. Software

Describe the software used to analyze the data in this study.

Graphpad Prism 6 and Microsoft Excel 2016

For manuscripts utilizing custom algorithms or software that are central to the paper but not yet described in the published literature, software must be made available to editors and reviewers upon request. We strongly encourage code deposition in a community repository (e.g. GitHub). *Nature Methods* [guidance for providing algorithms and software for publication](#) provides further information on this topic.

► Materials and reagents

Policy information about [availability of materials](#)

8. Materials availability

Indicate whether there are restrictions on availability of unique materials or if these materials are only available for distribution by a for-profit company.

All the materials are commercially available and materials generated by us (KO cell lines et al.) will be available upon request.

9. Antibodies

Describe the antibodies used and how they were validated for use in the system under study (i.e. assay and species).

This was described in the Methods.

10. Eukaryotic cell lines

a. State the source of each eukaryotic cell line used.

This was described in the Methods.

b. Describe the method of cell line authentication used.

This was described in the Methods.

c. Report whether the cell lines were tested for mycoplasma contamination.

This was described in the Methods.

d. If any of the cell lines used are listed in the database of commonly misidentified cell lines maintained by [ICLAC](#), provide a scientific rationale for their use.

Not applicable.

► Animals and human research participants

Policy information about [studies involving animals](#); when reporting animal research, follow the [ARRIVE guidelines](#)

11. Description of research animals

Provide details on animals and/or animal-derived materials used in the study.

This was described in the Methods.

Policy information about [studies involving human research participants](#)

12. Description of human research participants

Describe the covariate-relevant population characteristics of the human research participants.

Description of human research participants was done in the Methods and description the covariate-relevant population characteristics is not applicable.